

Isobar-doorway model for coherent π^0 photoproduction

A. N. Saharia and R. M. Woloshyn

TRIUMF, Vancouver, British Columbia, Canada V6T 2A3

(Received 1 July 1980)

The isobar-doorway model for pion-nucleus interaction is extended to coherent π^0 photoproduction. The modifications to the transition operator due to many-body effects are shown to be the same as those in the optical potential. Nonlocality associated with isobar propagation, recoil corrections, and an off-shell extrapolation of the $\pi N\Delta$ vertex are included. The calculated cross sections are found to be in good agreement with the existing data.

[NUCLEAR REACTIONS Coherent π^0 photoproduction; isobar doorway; optical potential model. Many-body modifications of the transition operator.]

I. INTRODUCTION

The inadequacy of the impulse approximation in generating the pion-nucleus optical potential in the 3-3 resonance region has been widely demonstrated. In Ref. 1 the isobar-doorway theory,² whose use introduces the isobars as explicit nuclear constituents, was used to parametrize the pion-nucleus optical potential. The advantage of such an approach is that it not only sums the higher-order terms in the multiple scattering series but also provides a means of including the many-body effects due to isobar dynamics in terms of a small number of phenomenological parameters. The parameters of the model in Ref. 1 were determined by comparing the angular distribution for elastic scattering with the experimental data. This model was later generalized to isospin non-zero targets,³ where it was found that the experimental charge exchange scattering cross section can be very simply reproduced by allowing the parameters to be different in different (pion-nucleus) isospin channels so as to take into account the isospin-dependent many-body modifications to the isobar propagator in the presence of the nuclear medium.

In this work we have extended the isobar-doorway model to π^0 photoproduction. It is well known that in the resonance energy region π^0 photoproduction on nucleons goes mainly through Δ production. Thus, any study of this reaction should include the effect of isobar nucleus dynamics not only in determining the pion-nucleus optical potential describing the final state interaction but also in the photoproduction operator. The isobar-doorway model provides a framework for doing so. We have considered only coherent π^0 photoproduction as, in this case, the doorway states, which are superpositions of Δ -(A-1) states diagonalizing the effective intermediate Hamiltonian, are the same as those for elastic scattering. The photoproduction operator is, therefore, completely

determined once the pion-nucleus optical potential is specified. This is discussed in detail in Sec. II. Following the parametrization^{1,2} of the optical potential, the transition operator is written in terms of a modified form factor and an energy shift and width. The corresponding parameters are no longer free but are determined by fitting elastic scattering. In Sec. III we give the details of such a determination of the parameters of the isobar-doorway model along with our results for elastic scattering on light nuclei. (The optical potential considered here contains certain refinements over the one of Ref. 1.) In Sec. IV we present our calculation for the (γ, π^0) reaction. Results of a distorted wave impulse approximation (DWIA) calculation, using a first-order optical potential, are also given. We compare our calculations with the (somewhat limited) existing data for $^{12}\text{C}(\gamma, \pi^0)^{12}\text{C}$ and $^4\text{He}(\gamma, \pi^0)^4\text{He}$. Finally in this section we discuss some earlier calculations of the process and compare them with ours. The conclusions are given in Sec. V.

II. FORMALISM

In the isobar-doorway theory the Hilbert space is divided into different subspaces, each with its own characteristics. We extend the P space to include all the asymptotic states with the target in its ground state—generated by the nonresonant part of the pion-nucleon and photon-nucleon interactions, D space containing Δ -(A-1) states, and Q space containing everything else. Using the projection operator algebra and making the doorway assumption $H_{PQ} = 0$ the effective Hamiltonian for the P space states is

$$\mathcal{H} = H_{PP} + H_{PD} \frac{1}{E - H_{DD} - H_{DQ} [1/(E - H_{QQ})] H_{QD}} H_{DP}, \quad (1)$$

so that the transition matrix is given by

$$\begin{aligned} \mathcal{T} &= \left(V^{\text{NR}} + H_{PD} \frac{1}{E - H_{DD} - H_{DQ} [1/(E - H_{QQ})] H_{QD}} H_{DP} \right) (1 + G_0 \mathcal{T}) \\ &= (1 + \mathcal{T} G_0) \left(V^{\text{NR}} + H_{PD} \frac{1}{E - H_{DD} - H_{DQ} [1/(E - H_{QQ})] H_{QD}} H_{DP} \right), \end{aligned} \quad (2)$$

where $G_0 = (E - H_0)^{-1}$ is the free Green's function and $V^{\text{NR}} = H_{PP} - H_0$ is the transition operator generated by interactions in P space. Equation (2) can alternatively be written as

$$\mathcal{T} = \mathcal{T}^{\text{NR}} + \langle \psi^{(-)} | H_{PD} \frac{1}{E - H_{DD} - H_{DQ} [1/(E - H_{QQ})] H_{QD} - H_{DP} [1/(E - H_{PP})] H_{PD}} H_{DP} | \psi^{(+)} \rangle, \quad (3)$$

where $\psi^{(+)}$ is the outgoing wave function generated by H_{PP} with \mathcal{T}^{NR} the corresponding T matrix:

$$(E - H_{PP}) \psi^{(+)} = 0 \text{ and } \mathcal{T}^{\text{NR}} = \langle \psi^{(-)} | \psi^{(+)} \rangle. \quad (4)$$

Although we shall not need the coupling potentials H_{PD} and H_{DP} , it is useful to write them explicitly

$$H_{PD} = H_{DP} = V_{\pi N\Delta} + V_{\gamma N\Delta} + \text{H.c.}, \quad (5a)$$

with

$$\langle \Delta | V_{\pi N\Delta} | N\pi_\alpha \rangle = \frac{f_{\pi N\Delta}}{m_\pi} \vec{S} \cdot \vec{q}^* T_{\alpha S}(q^*) \quad (5b)$$

and

$$\langle \Delta | V_{\gamma N\Delta} | N\gamma \rangle = \frac{f_{\gamma N\Delta}}{m_\pi} \vec{\epsilon} \cdot \vec{k}^* \times \vec{S} T_3, \quad (5c)$$

where q^* and k^* are the relative momenta for pion-nucleon and photon-nucleon systems, respectively, $\vec{\epsilon}$ the photon polarization vector, α the pion isospin and \vec{S} and \vec{T} the spin and isospin transition operators between spin and isospin $\frac{1}{2}$ and $\frac{3}{2}$.

In case the target is a nucleon, Eq. (3) reduces to

$$t_{\pi\pi} = t_{\pi\pi}^{\text{NR}} + \frac{\langle N\pi | V_{\pi N\Delta} | \Delta \rangle \langle \Delta | V_{\pi N\Delta} | N\pi \rangle}{E - M_\Delta + i\Gamma_\Delta/2} \quad (6a)$$

for pion-nucleon scattering and

$$t_{\gamma\pi} = t_{\gamma\pi}^{\text{NR}} + \frac{\langle N\pi | V_{\pi N\Delta} | \Delta \rangle \langle \Delta | V_{\gamma N\Delta} | N\pi \rangle}{E - M_\Delta + i\Gamma_\Delta/2} \quad (6b)$$

for pion photoproduction. In Eq. (6), M_Δ and Γ_Δ are the physical mass and width of the isobar given by

$$\begin{aligned} (E - M_\Delta + i\Gamma_\Delta/2) \\ = \left\langle \Delta \left| E - H_{DD} - H_{DP} \frac{1}{E^* - H_{PP}} H_{PD} \right| \Delta \right\rangle. \end{aligned} \quad (7)$$

In writing Eq. (6) we have assumed that in the energy region of interest the coupling of the nucleon to other mesons can be neglected (although we can include their contributions very easily).

For a nuclear target the T matrix can be evaluated² by introducing a complete set of states $|D_i\rangle$ which diagonalize the energy denominator of Eq.

(3):

$$\mathcal{T} = \mathcal{T}^{\text{NR}} + \sum_i \frac{\langle \psi^{(-)} | H_{PD} | D_i \rangle \langle D_i | H_{DP} | \psi^{(+)} \rangle}{E - E_{D_i} - (\epsilon_i^{\text{e}1} + \epsilon_i^{\text{i}1n}) + i(\Gamma_i^{\text{e}1} + \Gamma_i^{\text{i}1n})/2} \quad (8)$$

The problem then reduces to evaluating the ϵ 's and Γ 's given by

$$\epsilon_i^{\text{e}1} - i\Gamma_i^{\text{e}1}/2 = \left\langle D_i \left| H_{DP} \frac{1}{E^* - H_{PP}} H_{PD} \right| D_i \right\rangle \quad (9a)$$

and

$$\epsilon_i^{\text{i}1n} - i\Gamma_i^{\text{i}1n}/2 = \left\langle D_i \left| H_{DQ} \frac{1}{E^* - H_{QQ}} H_{QD} \right| D_i \right\rangle. \quad (9b)$$

This is the starting point of various calculations in recent years^{2,4-9} which take into account the isobar degree of freedom in a T -matrix formulation of the isobar-doorway model.

We, however, prefer to evaluate the transition operator [the quantity in square brackets in Eq. (2)] first and then calculate the T matrix. For pion elastic scattering the transition operator is just the optical potential. We evaluate it by introducing a complete set of states $|D_i\rangle$ which diagonalize the energy denominator in Eq. (2),

$$\begin{aligned} \langle \vec{q}' | V_{\text{opt}} | \vec{q} \rangle &= \langle \vec{q}' | V_{\text{opt}}^{\text{NR}} | \vec{q} \rangle \\ &+ \sum_i \frac{(E - M_\Delta + i\Gamma_\Delta/2)}{E - E_i^{\text{i}1n} + i\Gamma_i^{\text{i}1n}/2} t_{\pi\pi}^R(\vec{q}', \vec{q}) F_i(\vec{q}', \vec{q}) \end{aligned} \quad (10)$$

where

$$E_i^{\text{i}1n} - i\Gamma_i^{\text{i}1n}/2 = \left\langle D_i \left| H_{DD} + H_{DQ} \frac{1}{E^* - H_{QQ}} H_{QD} \right| D_i \right\rangle, \quad (11)$$

and we have used Eq. (6a) to write $V_{\pi N\Delta} V_{\pi N\Delta} = (E - M_\Delta + i\Gamma_\Delta/2) t_{\pi\pi}^R$, $t_{\pi\pi}^R$ being the pion-nucleon scattering amplitude in the 3-3 channel. The modified nuclear form factor $F_i(\vec{q}', \vec{q})$ is given by

$$\begin{aligned} F_i(\vec{q}', \vec{q}) &= \sum_N \int \phi_N^*(\vec{p}') \rho_\Delta^i(\vec{p}' + \vec{q}', \vec{p} + \vec{q}) \\ &\times \phi_N(\vec{p}) d^3p' d^3p \end{aligned} \quad (12)$$

with

$$\rho_{\Delta}^i(\vec{p}' + \vec{q}', \vec{p} + \vec{q}) = \phi_{\Delta}^i(\vec{p}' + \vec{q}') \phi_{\Delta}^{i*}(\vec{p} + \vec{q}), \quad (13)$$

ϕ_{Δ}^i being the wave function of the Δ in doorway state $|D_i\rangle$. The pion-nucleus scattering T matrix is then given by

$$\mathcal{T}_{\pi\pi} = (1 + \mathcal{T}G_0)V_{\text{opt}} \equiv \Omega V_{\text{opt}}. \quad (14)$$

For coherent π^0 photoproduction the transition operator can be evaluated in a similar way. Proceeding exactly as for the optical potential we get

$$\begin{aligned} \langle \vec{q} | \hat{t} | \vec{k} \rangle &= \langle \vec{q} | \hat{t}_{NR} | \vec{k} \rangle \\ &+ \sum_i \frac{(E - M_{\Delta} + i\Gamma_{\Delta}/2)}{E - E_i^{\text{in}} + i\Gamma_{D_i}^{\text{in}}/2} t_{\gamma\pi^0}^R(\vec{q}, \vec{k}) F_i(\vec{q}, \vec{k}), \end{aligned} \quad (15)$$

where we have used Eq. (6b) to write $V_{\pi N \Delta}^* V_{\gamma N \Delta} = (E - M_{\Delta} + i\Gamma_{\Delta}/2)t_{\gamma\pi^0}^R$. The pion photoproduction amplitude is then given by

$$\mathcal{T}_{\gamma\pi^0} = (1 + \mathcal{T}G_0)\hat{t} = \Omega \hat{t}. \quad (16)$$

The quantities E_i^{in} , Γ_i^{in} , and F_i occurring in Eq. (15) are exactly the same as in Eq. (10). Although the photon will in general couple to all the doorway states, the sum in Eq. (15) is restricted to only those occurring for elastic scattering as they have to have appropriate quantum numbers to couple to the final state of π^0 and the nuclear ground state. Thus to include many-body isobar effects in the (γ, π^0) reaction we have to modify the isobar propagator in exactly the same way as for the optical potential. This is shown schematically in Fig. 1.

A similar philosophy was adopted by Koch and Moniz⁹ in calculating the (γ, π^0) cross section using a T -matrix formulation of the isobar-doorway model. These authors correctly emphasize the relationship of coherent π^0 photoproduction to the off-shell π -nucleus T matrix. This is all the more apparent here as the transition operator is related

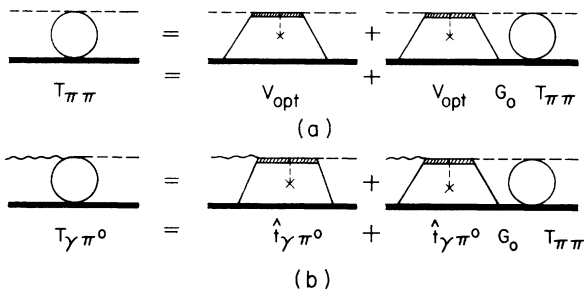


FIG. 1. Diagrammatical representation of pion elastic scattering and π^0 photoproduction in the isobar-doorway model. The interaction ---x represents all many-body modifications to the isobar propagator except those due to coupling to P space.

to the optical potential. The latter defines the off-shell as well as the on-shell pion-nucleus interaction. However, the implication in Ref. 9 that the off-shell behavior probed by (γ, π^0) is given by the off-diagonal elements of the Δ -hole propagator is a consequence of the model used to evaluate $G_{\Delta h}$. If we use the states $|D_i\rangle$ which diagonalize $H_{\Delta h}$ [see Eq. (8)] rather than the tridiagonal basis of Ref. 9, both elastic scattering and π^0 photoproduction would be given by the diagonal matrix elements $\langle D_i | G_{\Delta h} | D_i \rangle$.

III. PION-NUCLEUS OPTICAL POTENTIAL

As pointed out in Ref. 1, the theoretical determination of the quantities E_i^{in} , Γ_i^{in} , and F_i requires not only a detailed understanding of the isobar dynamics so as to construct the doorway states but also the coupling of doorway states to the complicated many-body states in the Q space. Rather than embarking on such involved calculations, a more phenomenological approach was taken in Ref. 1, i.e., to parametrize the optical potential given by Eq. (10).

For the nonresonant part we use the first-order optical potential¹⁰ with the interaction in the pion-nucleon 3-3 channel switched off. For the contribution of the pion-nucleon 3-3 channel we assume that the width Γ_i of the doorway states is larger than the average separation energy $E_i - E_{i\pm 1}$ so that the energy denominator in Eq. (10) can be replaced by an average over the contributing states. The resonant part of the optical potential is then given by

$$\begin{aligned} \langle \vec{q}' | V_{\text{opt}}^R | \vec{q} \rangle &= \frac{1}{E - M_{\Delta} - \Delta E + i\beta\Gamma_{\Delta}/2} \\ &\times [(E - M_{\Delta} + i\Gamma_{\Delta}/2)t_{\pi\pi}^R(\vec{q}', \vec{q}, E)F(\lambda; \vec{q}', \vec{q})] \end{aligned} \quad (17)$$

with $F(\lambda; \vec{q}', \vec{q})$ as the modified nuclear form factor which takes into account the nonlocality associated with Δ propagation in the nucleus. In modeling the form factor, the isobar density matrix was parametrized in Ref. 1 as

$$\rho_{\Delta}(\vec{r}_1, \vec{r}_2) = \sum_i \phi_i^{\Delta}(\vec{r}_1) \phi_i^{\Delta*}(\vec{r}_2) = \frac{e^{-\frac{(\vec{r}_1 - \vec{r}_2)^2}{\lambda^2}}}{(\pi\lambda^2)^{3/2}}. \quad (18)$$

The form factor F is then evaluated for p -shell nuclei using harmonic oscillator wave functions,

$$\begin{aligned} F(\lambda; \vec{q}', \vec{q}) &= 2 \left\{ 1 + \alpha \left[\left(\frac{3}{2} - \frac{Q^2 c^2}{4} \right) - \frac{\beta^2}{c^2 4} \left(\frac{3}{2} - \frac{K^2 \beta^2}{4} \right) \right] \right\} \\ &\times e^{-Q^2 c^2 / 4} e^{-K^2 \beta^2 / 4} F_{c.m.}(Q) \end{aligned} \quad (19)$$

with $\vec{Q} = \vec{q}' - \vec{q}$, $\vec{K} = (\vec{q} + \vec{q}')/2$, $\beta^2 = c^2 \lambda^2 / (c^2 + \lambda^2/4)$, $\alpha = (N - 2)/3[(Z - 2)/3]$ for neutrons (protons) and

c the harmonic oscillator parameter. $F_{c.m.}(Q)$ is the correction due to the center of mass motion of the target which we take from the static limit¹¹ to be $\exp(Q^2 c^2/4A)$.

The choice of nonlocality given by Eq. (18) was motivated by the fact that under closure ρ_Δ reduces to $\delta^3(\vec{r}_1 - \vec{r}_2)$, a limit conveniently obtained by taking $\lambda=0$. However, such a choice [ρ_Δ being a function of $(\vec{r}_1 - \vec{r}_2)$ only] necessarily implies that we are including only the situation where the three-momentum of the isobar is the same in the initial and final doorway states.¹² In general this need not be true. To allow for the momentum spread introduced by interactions of the isobar with the nuclear medium, we generalize Eq. (18) to

$$F(\lambda; \vec{q}', \vec{q}) = 2 \left\{ 1 + \alpha \left[\left(\frac{3}{2} - \frac{Q^2 c^2}{4} \right) - \frac{\beta_2^2}{4c^2} \left(\frac{3}{2} - \frac{K^2 \beta_2^2}{4} \right) \right] \right\} \times e^{-Q^2 \beta_1^2/4} e^{-K^2 \beta_2^2/4} F_{c.m.}(Q) \quad (20)$$

with

$$\beta_1^2 = \frac{c^2 \lambda_1^2}{c^2 + \lambda_1^2} \text{ and } \beta_2^2 = \frac{c^2 \lambda_2^2}{c^2 + \lambda_2^2/4}, \quad (21)$$

where λ_1 and λ_2 are given by a single (dimensionless) parameter λ ,

$$\lambda_1 = \frac{1}{q_0 \lambda} \text{ and } \lambda_2 = \frac{\lambda}{q_0}, \quad (22)$$

with q_0 as the on-shell relative momentum for the pion-nucleus system, so that the closure limit is again given by $\lambda=0$.

The parameters of the isobar-doorway model, the energy shift ΔE , width parameter β , and nonlocality parameter λ take into account not only various many-body effects like true absorption, Pauli blocking, and inelastic scattering but also the effect of Fermi motion. The reason is that the numerator in Eq. (17) is just the product $V_{\pi N \Delta}^* V_{\pi N \Delta}$ averaged over the nucleon and Δ wave function and hence contains no rapid energy variation. Using an appropriate transformation (including the "angle transformation") from π -nucleon c. m. frame to π -nucleus c. m. frame, the only approximation used in factorizing $t_{\pi\pi}^R$ out of the integral is that the off-shell extrapolation factor $g(q^*)g(q^{*'})/g^2(q_0^*)$ is a slowly varying function of the momenta.

In general the parameters ΔE and β would depend on the pion-nucleus quantum numbers like l , J , T , etc. In Ref. 1 this channel-dependence was included for spin-zero isospin-zero targets by taking a Fermi cutoff for ΔE_l and $(\beta_l - 1)$,

$$\Delta E_l = \frac{\Delta E}{1 + \exp[(l - l_0)/\delta l_0]} \quad (23a)$$

and

$$\beta_l = 1 + \frac{(\beta - 1)}{1 + \exp[(l - l_0)/\delta l_0]}, \quad (23b)$$

where $l_0 = q_0 R$ and $\delta l_0 = q_0 t$, R and t being nucleus radius and surface thickness, respectively. However, in view of the large width of the doorway states, it is not unreasonable to take ΔE and β to be channel-independent quantities. It should be pointed out, however, that even a channel-independent parametrization of the optical potential in the isobar-doorway model does not correspond to taking the eigenenergies of the (projected) total Hamiltonian in the D space $H_{DD} + H_{DQ}[1/(E - H_{QQ})]H_{QD} + H_{DP}[1/(E - H_{PP})]H_{PD}$ as channel-independent quantities. These eigenenergies include elastic widths and shifts which in general depend on angular momentum very strongly.

The parameters of the model are determined by fitting elastic scattering data in the resonance energy region. The harmonic oscillator parameter c is taken as 1.36, 1.64, and 1.77 fm for ${}^4\text{He}$, ${}^{12}\text{C}$, and ${}^{16}\text{O}$, respectively, as determined by electron scattering experiments.^{13,14} A typical fit in the resonance energy region is shown in Fig. 2 along with the predictions of the code PIPIT.¹⁰ The

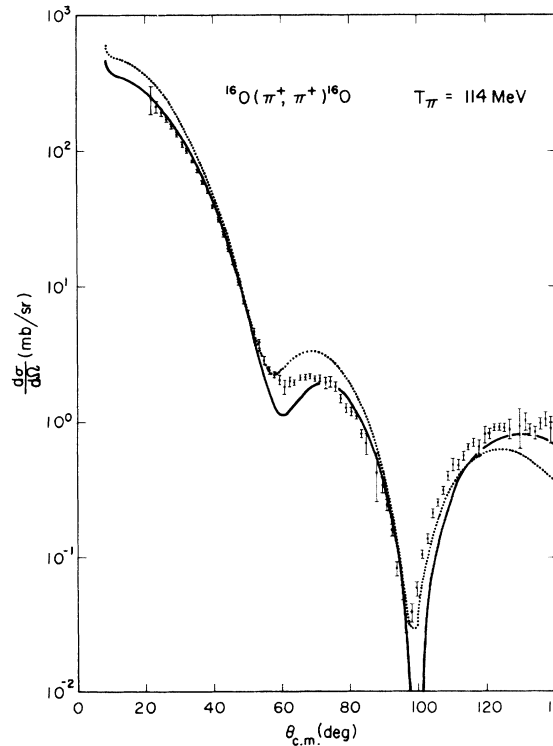


FIG. 2. A typical fit pion elastic scattering. ${}^{16}\text{O}(\pi^+, \pi^+){}^{16}\text{O}$ at pion kinetic energy of 114 MeV: dotted curve—prediction of the first order optical potential (Ref. 10); solid curve—channel-independent isobar-doorway model. The data are taken from Ref. 15.

TABLE I. Parameters of the IDM for $\pi^-^{16}\text{O}$ scattering. Quantities in parentheses correspond to channel-dependent IDM.

T_r (MeV)	ΔE (MeV)	β	λ
114 ^a	4.07 (0.023)	1.264 (1.538)	0.38 (0.373)
163 ^a	0.201 (-7.7)	1.12 (1.333)	0.329 (0.327)
240 ^a	4.26 (11.99)	1.2 (1.168)	0.176 (0.135)

^aData from Ref. 15.

parameters of the channel-independent isobar-doorway model are given in Tables I–III. For ^{16}O the parameters of the channel-dependent IDM are given in parentheses in Table I. In general, very good fits to the data were obtained with χ^2 ranging from 0.5 to 1.5 per degree of freedom. The parameters showed a large error and a strong correlation at the minimum χ^2 . However, no effort was made to determine the correlation matrix due to the large amount of computer time taken by the momentum space code.

IV. π^0 PHOTOPRODUCTION

Making the same approximations as for the optical potential we write the transition operator as

$$\langle \vec{q} | \hat{t} | \vec{k} \rangle = t_{\gamma\pi^0}^{NR}(\vec{q}, \vec{k}, E) \rho(\vec{q} - \vec{k}) + \frac{1}{E - M_\Delta - \Delta E + i\beta\Gamma_\Delta/2} \times [(E - M_\Delta + i\Gamma_\Delta/2) t_{\gamma\pi^0}^R(\vec{q}, \vec{k}, E) F(\lambda; \vec{q}, \vec{k})], \quad (24)$$

where not only the quantities ΔE and β are the same as for the optical potential but also the form factor F is the same. The reason for this, as discussed earlier, is that in coherent π^0 photoproduction the same doorway states occur as in elastic scattering and the quantities ΔE , β , and F are

TABLE II. Parameters of the IDM for $\pi^-^{12}\text{C}$ scattering.

T_r (MeV)	ΔE (MeV)	β	λ
120 ^a	19.9	1.26	0.368
148 ^b	16.59	1.094	0.400
150 ^a	19.87	1.065	0.45
162 ^b	-3.7	1.146	0.462
180 ^a	12.59	1.186	0.336
200 ^a	16.14	1.263	0.270
230 ^a	19.9	1.160	0.112

^aData from Ref. 16.

^bData from Ref. 17.

TABLE III. Parameters of the IDM for $\pi^-^4\text{He}$ scattering.

T_r (MeV)	ΔE (MeV)	β	λ
110 ^a	14.42	1.183	0.32
150 ^a	14.42	1.0417	0.32
180 ^a	0.87	1.055	0.113
220 ^a	0.87	1.055	0.079

^aData from Ref. 18.

the property of these doorway states. The only additional input to Eq. (24) is the amplitudes $t_{\gamma\pi^0}^{NR}$ and $t_{\gamma\pi^0}^R$ which we take as

$$t_{\gamma\pi^0}^{NR} = \vec{\epsilon} \cdot \frac{\vec{k}^* \times \vec{q}^*}{k^* q^*} M^{NR} \quad (25)$$

and

$$t_{\gamma\pi^0}^R = \vec{\epsilon} \cdot \frac{\vec{k}^* \times \vec{q}^*}{k^* q^*} M^R \frac{f(q^*)}{f(q_0^*)}$$

with M^{NR} and M^R taken from multipole analysis of Pfeil and Schwela¹⁹ and f , the off-shell form factor. Here, \vec{k}^* and \vec{q}^* are the relative momenta in the c.m. frame for the photon-nucleon and pion-nucleon systems, respectively,

$$\vec{k}^* = \frac{M_N}{\sqrt{S_{\gamma N}}} (\vec{k} - a\vec{p}), \quad (26)$$

$$\vec{q}^* = \frac{M_N}{\sqrt{S_{\pi N}}} (\vec{q} - b\vec{p}),$$

where a and b are evaluated by making a frozen-nucleon approximation.

Although the transition operator Eq. (24) looks like the pion-nucleus optical potential because of the transverse nature of the photon field, there are some important differences between the two when we include the recoil corrections. We discuss these differences in detail here. (Most of these considerations apply to both the impulse approximation calculations and the isobar-doorway model calculations.)

A. Phase space and flux factors

This correction is the same as for the optical potential. The two-body amplitude in the pion-nucleus c.m. frame is related to the amplitude in the pion-nucleon c.m. frame by

$$t(\vec{q}, \vec{k}, E) = \left[\frac{E_\pi(q^*) E_\gamma(k^*) E_N(q^*) E_N(k^*)}{E_\pi(q) E_\gamma(k) E_N(q/A) E_N(k/A)} \right]^{1/2} \times t(\vec{q}^*, \vec{k}^*, \sqrt{S_{\pi N}}), \quad (27)$$

where we have used the frozen nucleus approximation to evaluate energies E_N in the pion-nucleus c.m. frame.

B. Recoil corrections and Fermi averaging

For the pion optical potential, inclusion of recoil corrections leads to the p wave in the pion-nucleon c.m. frame feeding into the s wave.¹⁰ Although there is no unique prescription for such an angle transformation, using the momentum-conserving form of the nonlocality we can show that

$$\sum_N \int \bar{q}^* \cdot \bar{q}' \phi_N^*(\bar{p} + \bar{q} - \bar{q}') \rho_\Delta(\bar{p} + \bar{q}) \phi_N(\bar{p}) d^3p \approx \frac{M_N^2}{S_{\pi N}} \left[\bar{q} \cdot \bar{q}' - \frac{b}{2} (\bar{q} - \bar{q}')^2 \right] F(\lambda; \bar{q}', \bar{q}), \quad (28)$$

where

$$\bar{q}^* = \frac{M_N}{\sqrt{S_{\pi N}}} (\bar{q} - b\bar{p})$$

and

$$\bar{q}'^* = \frac{M_N}{\sqrt{S_{\pi N}}} [\bar{q}' - b(\bar{p} + \bar{q} - \bar{q}')]. \quad (29)$$

Thus, at forward angles, where the elastic scattering cross section is large, the contribution of the correction terms being proportional to $(\bar{q} - \bar{q}')^2$ is small. However, for the π^0 -photoproduction operator, similar estimates give

$$\sum_N \int \bar{k}^* \times \bar{q}^* \phi_N^*(\bar{q} + \bar{k} - \bar{q}) \rho_\Delta(\bar{p} + \bar{k}) \phi_N(\bar{p}) d^3p \approx \frac{M_N^2}{S_{\pi N}} \left(1 + \frac{q}{2} + \frac{b}{2} - \frac{ab}{2} \right) \bar{k} \times \bar{q} F(\lambda; \bar{q}, \bar{k}). \quad (30)$$

Thus the recoil corrections also go as $\bar{k} \times \bar{q}$. Taking $a \sim k_0/M_N$ and $b \sim \omega_q/M_N$ we see that these amount to about a 25% increase in cross section over the whole angular range. Again, as in the case of the optical potential, this gives us a way of including Fermi averaging, as the only quantity we are factorizing out in writing Eq. (24) is the off-shell extrapolation factor $f(q^*)/f(q_0^*)$.

C. Center-of-mass motion

We include this in the same way as for the optical potential by multiplying the form factor with $F_{c.m.}(\bar{q} - \bar{k}) = \exp[(\bar{k} - \bar{q})^2 c^2 / 4A]$.

D. Off-shell extrapolation

Whereas for constructing the pion optical potential we use the Londergan-McVoy-Moniz (LMM)²⁰ off-shell extrapolation for the $\pi N T$ matrix, for the $(\gamma, \pi^0) T$ matrix we use the form factor suggested by Blomqvist and Laget,²¹

$$f(q^*) = \left(\frac{1}{1 + r_0^2 q^{*2}} \right)^{1/2}, \quad (31)$$

with $r_0 = 0.00552 \text{ MeV}^{-1}$. Of course other dynamical models would lead to a different off-shell extrapolation. Fortunately, the results are not very sensitive to the actual value of the cutoff parameter, as can be seen from Fig. 3, where we compare the full calculation with that corresponding to the zero range calculation: $f(q^*)/f(q_0^*) = 1$. The effect of putting the form factor at the $\pi N \Delta$ vertex is to lower the (γ, π^0) cross section by a small amount.

Also shown in Fig. 3 is the result of doing an on-shell calculation by taking the distortion operator $\Omega(\bar{q}, \bar{q}') = \Omega(\bar{q}, \bar{q}) \delta(\bar{q} - \bar{q}')$. In this case the cross section is lower than that for the full calculation. This implies that the distortion operator not only provides a damping mechanism but also a focusing effect.

The calculations are done using a multipole expansion of the π^0 -photoproduction amplitude τ_{γ, π^0} . Taking the pion distortion operator as

$$\langle \bar{q}' | \Omega | \bar{q} \rangle = \sum_{i_m} \frac{\Omega_i(q', q)}{q^2} Y_{i_m}(\hat{q}') Y_{i_m}^*(\hat{q}) \quad (32)$$

and

$$F(\lambda; \bar{q}' \bar{k}) = \sum_{i_m} F_i(q', k) Y_{i_m}^*(\hat{q}') Y_{i_m}(\hat{k}) \quad (33)$$

and putting in various kinematic effects discussed here we get

$$\tau_{\gamma, \pi^0} = \tau_{\gamma, \pi^0}^{NR} + \tau_{\gamma, \pi^0}^R, \quad (34)$$

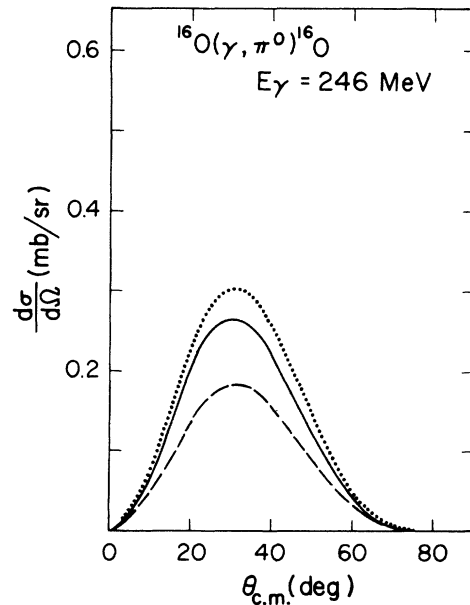


FIG. 3. Effect of including the off-shell form factor at the $\pi N \Delta$ vertex: solid curve—full calculation; dotted curve—no form factor. The dashed curve results from an on-shell approximation (see text).

where

$$T_{\gamma\pi^0}^R = \mathcal{E} M'^R \sum_J (2\pi)^{1/2} \left[\frac{J(J+1)}{2J+1} \right]^{1/2} T_{jm}^R Y_{JM}(\hat{q}) \quad (35)$$

with

$$T_{JM}^R = M \int \frac{q'}{q} [F_{J-1}(q', k) - F_{J+1}(q', k)] \times \frac{f(q'^*)}{f(q_0^*)} \Omega_J(q', q) dq, \quad (36)$$

$$M'^R = \left\{ \left[\frac{S_{\pi N} E_A(k) E_A(q)}{S_{\pi A} E_N(k/A) E_N(q/A)} \right]^{1/2} \times \left(1 + \frac{b}{2} + \frac{a}{2} - \frac{ab}{2} \right) \frac{M_N^2}{S_{\pi N}} \frac{kq}{k^* q^*} \right\} M^R(q^*, k^*, \sqrt{S_{\pi N}}), \quad (37)$$

and

$$\mathcal{E} = \frac{E - M_\Delta + i\Gamma_\Delta/2}{E - M_\Delta - \Delta E + i\beta\Gamma_\Delta/2}, \quad (38)$$

M being the photon polarization and $S_{\pi A}$ the invariant mass of the pion-nucleus system. The impulse approximation (which we use for the nonresonant part) is obtained by taking \mathcal{E} as 1 and $F_i(q, k)$ as $\rho_i(q, k)$ —the angular decomposition of the nuclear density. The photoproduction cross section is then given by

$$\frac{d\sigma}{d\Omega} = \frac{1}{2} \sum_\lambda \frac{q}{k} |T_{\gamma\pi^0}^R|^2. \quad (39)$$

In the absence of the corrections A and B , the quantity in square brackets in Eq. (37) would be just unity. Putting in these recoil corrections increases the cross section by a factor of 2 to 2.5 in the resonance energy region.²² These corrections were neglected in the earlier calculations of Saunders²³ and Woloshyn⁶. The reasonable agreement of the PWIA calculations of Refs. 23 and 6 with the experimental data of Davidson,²⁴ as reported by Saunders, can at most be described as accidental.

In Fig. 4(a) we show the comparison of the plane wave calculations with the distorted wave calculation for the channel-independent IDM at $E_\gamma = 254$ MeV. The calculations shown are (a) PWIA where no distortion and no modification to the transition operator is included, (b) PWMLA where no distortion is included but the modifications to the transition operator because of isobar dynamics are included, (c) DWIA where full distortion effects are included but no modifications to the transition operator are included, and (d) the full calculation where the many-body effects are included so as to modify both the transition operator and the distorting potential. As can be seen, the operator modi-

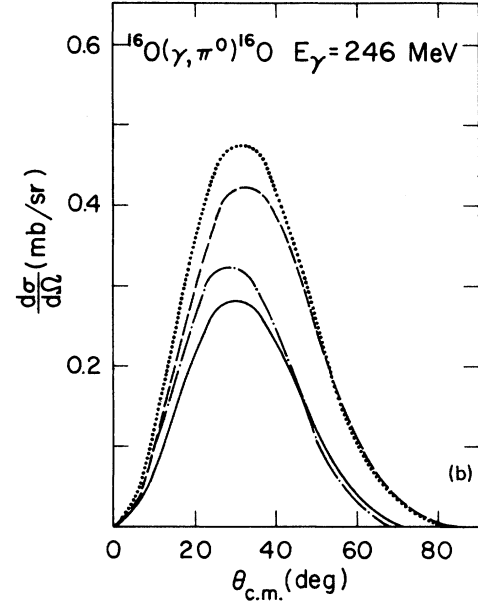
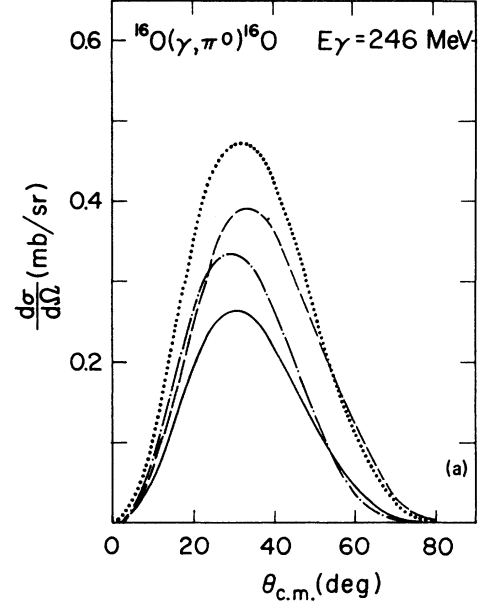


FIG. 4. (a) Effect of including many-body effects in the optical potential and the transition operator on $^{16}\text{O}(\gamma, \pi^0)^{16}\text{O}$ for the channel-independent isobar-doorway model: dotted curve—plane wave impulse approximation calculation; dashed curve—plane wave calculation with the transition operator modified; dash-dot curve—distorted wave impulse approximation calculation where many-body effects are included only in the optical potential; solid curve—full calculation where the many-body effects are included both in the transition operator and the optical potential. (b) Same as (a) except for the channel-dependent isobar-doorway model.

fication is very significant. Thus, in this energy region a DWIA calculation where the many-body effects are included only in the pion distortion operator would have limited validity.

In Fig. 4(b) we show the similar results for channel-dependent IDM (where we allow the parameters ΔE and β to be l dependent). It is interest-

ing to note that, although the isobar effects in the operator modification and the distorting potential are different for the two cases, the final results are very nearly the same. This can be easily understood by looking at the elastic scattering amplitude and π^0 -photoproduction amplitude. Neglecting constants, these are essentially given by

$$\begin{aligned} \langle \vec{q} | \tau_{rr} | \vec{q}' \rangle &= \int \langle \vec{q}'' | V_{opt} | \vec{q}' \rangle \Omega(\vec{q}, \vec{q}'') d^3 q'' \\ &\approx \frac{g(q^{*'})}{g^2(q_0^*)} \vec{q}' \cdot \left[\int \delta \vec{q}'' g(q^{*''}) F(\vec{q}'', \vec{q}') \Omega(\vec{q}, \vec{q}'') d^3 q'' \right] \approx \frac{g(q^{*'})}{g^2(q_0^*)} \vec{q}' \cdot \vec{I}(\vec{q}) \end{aligned} \quad (40)$$

and

$$\begin{aligned} \langle \vec{q} | \tau_{r0} | \vec{k} \rangle &= \int \langle q'' | \bar{t}_{r0} | k \rangle \Omega(\vec{q}, \vec{q}'') d^3 q'' \\ &\approx \frac{1}{f(q_0^*)} \vec{\epsilon} \times \vec{k} \cdot \left[\int \delta \vec{q}'' f(q^{*''}) F(\vec{q}'', \vec{k}) \Omega(\vec{q}, \vec{q}'') d^3 q'' \right] \approx \frac{1}{f(q_0^*)} \vec{\epsilon} \times \vec{k} \cdot \vec{I}(q), \end{aligned} \quad (41)$$

where $\vec{I}[\vec{I}']$ is the integral in the square bracket in Eq. (40) [(41)]. To the extent that $g \approx f$ and $q' \approx k$, $\vec{I}(q) \approx \vec{I}'(q)$. Thus, in any model where the many-body effects are parametrized through the optical potential, the quantity I is what is determined by fitting the elastic scattering. The two parametrizations of the isobar-doorway model which lead to the same elastic scattering will therefore give the same $\vec{I}(\vec{q})$ and hence the same (γ, π^0) cross section.

In Figs. 5 and 6 we give our predictions for the angular distribution for π^0 photoproduction on ^{12}C and ^{16}O along with standard DWIA calculations (using PIPIT¹⁰ wave functions). In Figs. 7 and 8, the corresponding integrated cross sections are given, together with those for PWIA. Whereas the angular distribution for the isobar-doorway model and DWIA are different at higher energies, the integrated cross sections are very close for the two calculations. The reason for this is that the differential cross section for the isobar-doorway model is slightly larger at larger angles (where $\sin\theta$ is larger) which compensates for the smaller value at the peak. Thus the experimental test for our model would be provided by measurement of both the differential and total cross section.

In Figs. 9, 10, and 11 we compare the predictions of the isobar-doorway model with the existing data^{24,25} for coherent (γ, π^0) reaction on ^{12}C and ^4He . Despite the suggestions⁹ that Davidson's data for $^{12}\text{C}(\gamma, \pi^0)^{12}\text{C}$ includes considerable contribution from noncoherent processes, we obtain rea-

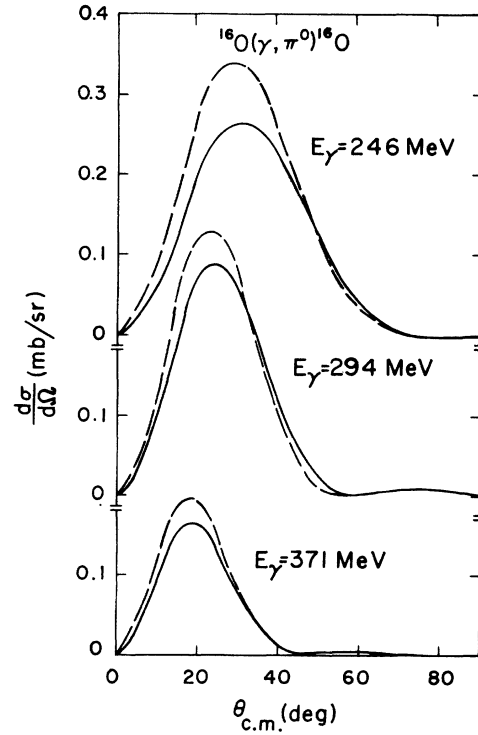


FIG. 5. Angular distributions for $^{16}\text{O}(\gamma, \pi^0)^{16}\text{O}$ at laboratory photon energies of 246, 294, and 371 MeV: dashed curve—DWIA calculation using PIPIT wave functions; solid curve—channel-independent isobar-doorway model.

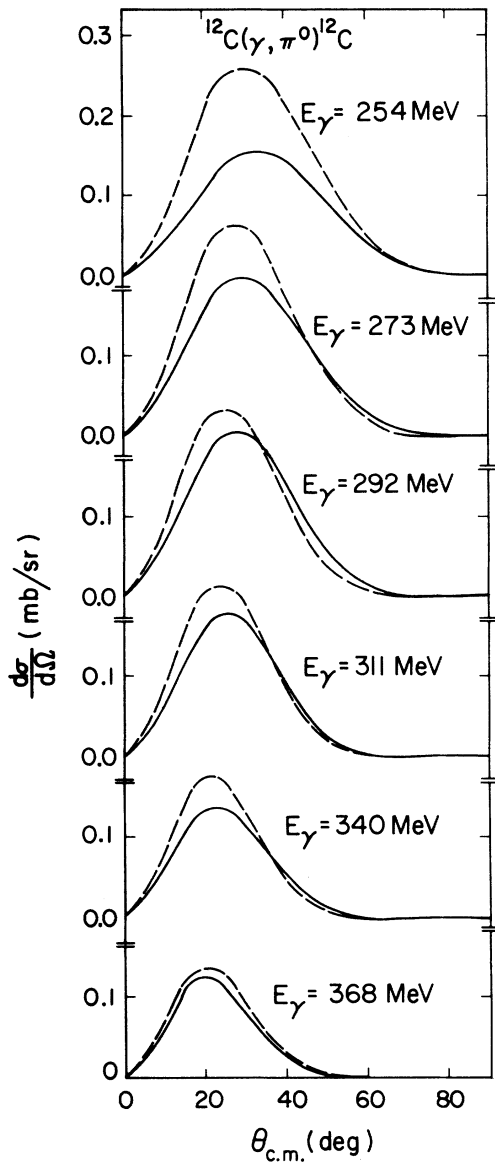


FIG. 6. Angular distributions for $^{12}\text{C}(\gamma, \pi^0)^{12}\text{C}$ at laboratory photon energies of 254, 273, 292, 311, 340, and 368 MeV: dashed curve—DWIA calculation using PIPIT wave functions; solid curve—channel-independent isobar-doorway model.

sonable agreement with it. As pointed out earlier, the conclusion reached by Saunders²³ that PWIA calculations describe the data fairly well may be due to neglect of various kinematic correction factors in that work. For $^4\text{He}(\gamma, \pi^0)^4\text{He}$, the agreement is reasonable despite limited amounts of data available in the resonance energy region.

Finally we compare our results with the calcu-

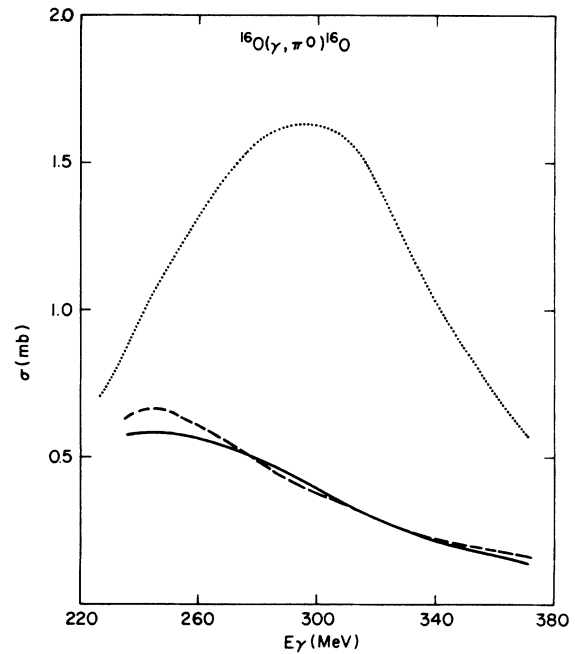


FIG. 7. Integrated cross section for $^{16}\text{O}(\gamma, \pi^0)^{16}\text{O}$ as a function of photon energy E_γ : dotted curve—PWIA calculation; dashed curve—DWIA calculation using the PIPIT wave function; solid curve—channel-independent isobar-doorway model.

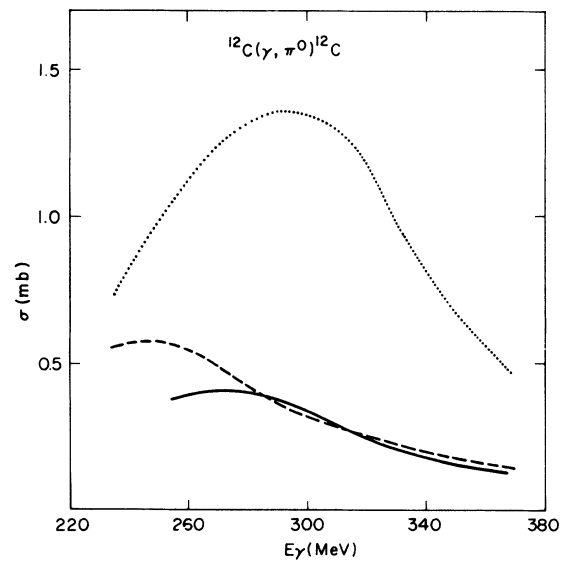


FIG. 8. Integrated cross section for $^{12}\text{C}(\gamma, \pi^0)^{12}\text{C}$ as a function of photon energy E_γ : dotted curve—PWIA calculation; dashed curve—DWIA calculation using the PIPIT wave function; solid curve—channel-independent isobar-doorway model.

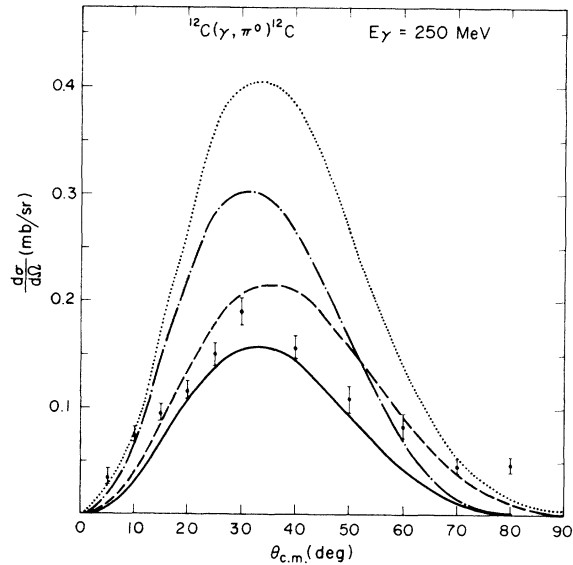


FIG. 9. Comparison of the channel-independent isobar-doorway model prediction for the angular distribution of $^{12}\text{C}(\gamma, \pi^0)^{12}\text{C}$ at photon energy of 250 MeV with the data of Davidson (Ref. 24). See Fig. 4 for the meaning of different curves.

lation of Koch and Moniz⁹ which included the same kinematic effects described in this section as well as effects due to isobar dynamics in a T -matrix formulation of the isobar-doorway model. The PWIA results of Ref. 9 for $^{16}\text{O}(\gamma, \pi^0)^{16}\text{O}$ are quite similar to those obtained here. Our distorted wave calculations, where many-body effects are included only in the optical potential but not in the transition operator (dashed-dot curves in Fig. 4), are also in close agreement with the DWIA results of Ref. 9. We attribute the ten to fifteen percent difference to differences in the models for the elementary (γ, π^0) process. Below photon energies of 300 MeV the final results are very different. A much larger reduction of the amplitude due to isobar modification in the production operator was found by Koch and Moniz and their final cross sections are about a factor of 2 smaller than ours. This difference probably reflects the ambiguity in the parametrization of the coupling to Q space which is treated differently in the two calculations.

V. CONCLUSIONS

We have shown that the many-body effects modifying the isobar propagator play an important role in determining the transition operator for (γ, π^0) reactions. Within an isobar-doorway model we show that the modifications to the transition operator for the coherent process are the same (neg-

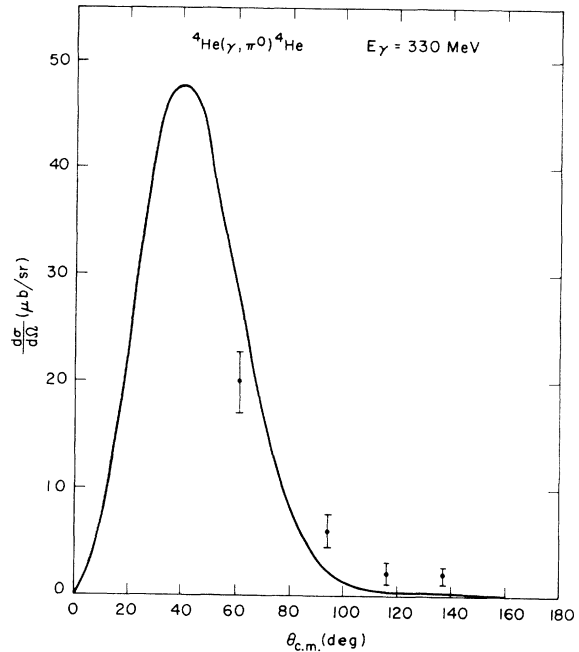


FIG. 10. Comparison of the channel-independent isobar-doorway model prediction for the angular distribution of $^4\text{He}(\gamma, \pi^0)^4\text{He}$ at photon energy 330 MeV with the data of Staples (Ref. 25).

lecting small recoil effects) as those to the pion-nucleus optical potential. The (γ, π^0) reaction therefore provides an unambiguous test of isobar-doorway models which require phenomenological information to describe pion elastic scattering.

In this paper we present results for coherent π^0 photoproduction on ^4He , ^{12}C , and ^{16}O for photons in the 200 to 380 MeV energy range. Our calculated photoproduction cross sections are not sensitive to the choice of a channel-dependent or channel-independent parametrization as long as the models are constrained to describe pion elastic scattering equally well. Also, the variations due to different off-shell extrapolations of the input multipole amplitudes are sufficiently small to permit a good test of the isobar-doorway models.

Our calculations are in good agreement with the limited existing data. More systematic measurements are needed to put our model to a more rigorous test and to distinguish between different approaches used to incorporate many-body effects in the pion-nucleus interactions.

ACKNOWLEDGMENTS

It is a pleasure to thank L. S. Kisslinger, J. H. Koch, and F. Lenz for helpful discussions. This work was supported in part by the Natural Sciences and Engineering Research Council of Canada.

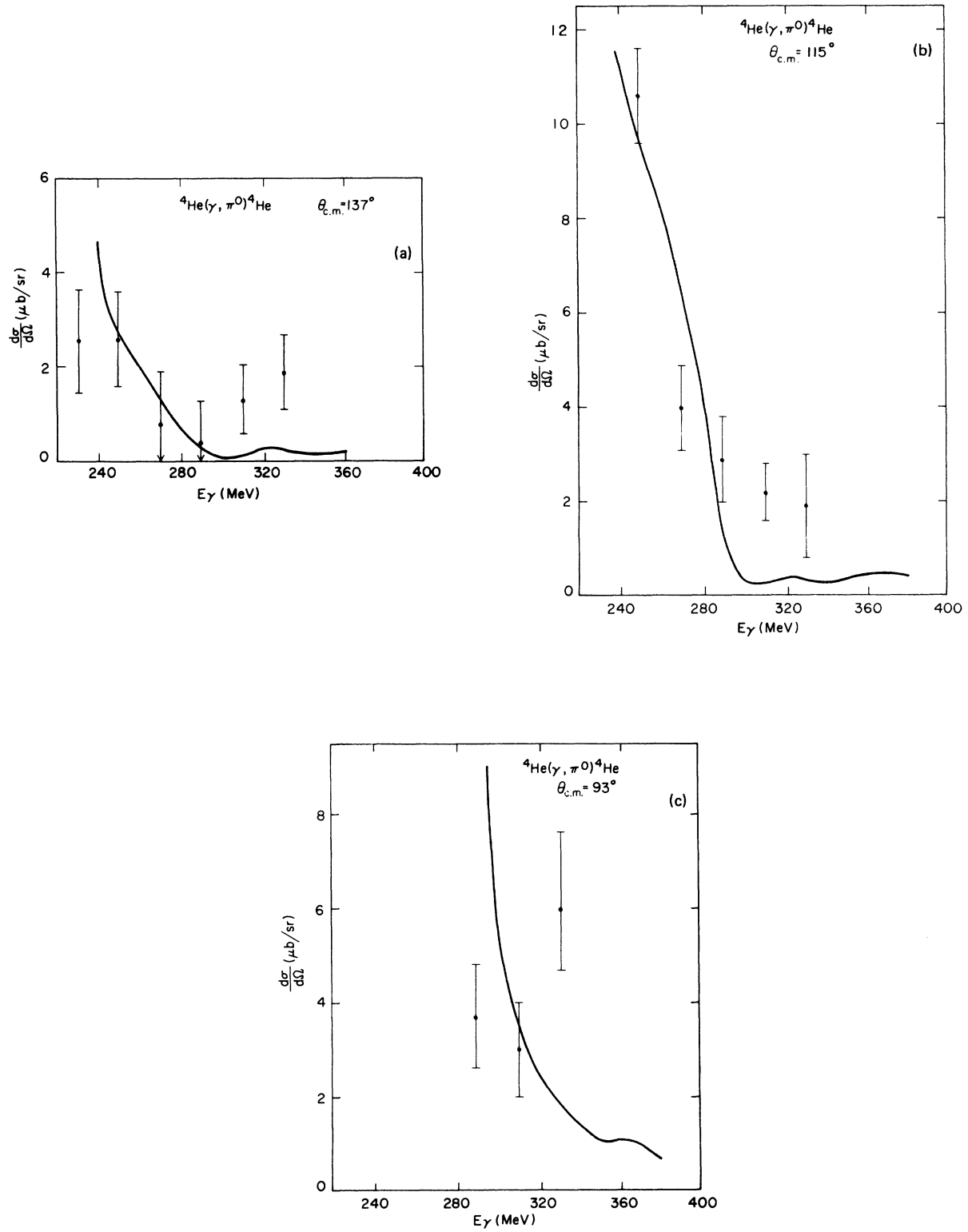


FIG. 11. (a) Comparison of the channel-independent isobar-doorway model calculation for the fixed angle c.m. differential cross section as a function of photon laboratory energy with the data of Staples (Ref. 25) at $\theta_{c.m.} = 137^\circ$. (b) Same as (a) except at $\theta_{c.m.} = 115^\circ$. (c) Same as (a) except at $\theta_{c.m.} = 93^\circ$.

- ¹L. S. Kisslinger and A. N. Saharia, TRIUMF Report No. TRI-PP-79-20; *Meson-Nuclear Physics—1976 (Carnegie-Mellon Conference)*, Proceedings of the International Topical Conference on Meson-Nuclear Physics, edited by P. D. Barnes, R. A. E. Eisenstein, and L. S. Kisslinger (AIP, New York, 1976), p. 184.
- ²L. S. Kisslinger and W. L. Wang, *Ann. Phys. (N.Y.)* **99**, 374 (1976).
- ³A. N. Saharia and R. M. Woloshyn, *Phys. Rev. C* **21**, 1111 (1980).
- ⁴M. Hirata, J. H. Koch, F. Lenz, and E. J. Moniz, *Ann. Phys. (N.Y.)* **120**, 205 (1979).
- ⁵K. Klingenberg, M. Dillig, and M. G. Huber, *Phys. Rev. Lett.* **41**, 387 (1978).
- ⁶R. M. Woloshyn, *Phys. Rev. C* **18**, 1056 (1978).
- ⁷N. Auerbach, *Phys. Rev. Lett.* **39**, 804 (1977).
- ⁸E. Oset and W. Weise, *Nucl. Phys.* **A329**, 365 (1979).
- ⁹J. H. Koch and E. J. Moniz, *Phys. Rev. C* **20**, 235 (1979).
- ¹⁰R. A. Eisenstein and F. Tabakin, *Comput. Phys. Commun.* **12**, 237 (1976).
- ¹¹L. L. Foldy and J. D. Walecka, *Ann. Phys. (N.Y.)* **54**, 447 (1969).
- ¹²We are thankful to Dr. Chi-Shiang Wu for pointing this out.
- ¹³T. W. Donnelly and G. E. Walker, *Phys. Rev. Lett.* **22**, 1121 (1969).
- ¹⁴R. F. Frosch, J. S. McCarthy, E. R. Rand, and M. R. Yearian, *Phys. Rev.* **160**, 874 (1967).
- ¹⁵J. P. Albanese, J. Arvieux, E. Boschitz, C. H. Q. Ingram, L. Pflug, C. Wiedner, and J. Zichy, *Phys. Lett.* **73B**, 119 (1978).
- ¹⁶F. Binon, P. Duteil, J. P. Garron, J. Gorres, L. Hugon, J.-P. Peigneux, C. Schmit, M. Spighel, and J.-P. Stroot, *Nucl. Phys.* **B17**, 168 (1970); F. Binon, V. Bobyr, P. Duteil, M. Gouanere, L. Hugon, J.-P. Peigneux, R. Renuart, C. Schmit, M. Spighel, and J.-P. Stroot, *ibid.* **B33**, 42 (1971).
- ¹⁷J. Piffaretti, R. Corfu, J.-P. Egger, P. Gretillat, C. Lunke, and E. Schwarz, *Phys. Lett.* **67B**, 289 (1977); J. Piffaretti, R. Corfu, J.-P. Egger, P. Gretillat, C. Lunke, E. Schwarz, C. Perrin, and B. M. Freedom, *ibid.* **71B**, 324 (1977).
- ¹⁸F. Binon, P. Duteil, M. Gouanere, L. Hugon, J. Jansen, J.-P. Lagnaux, H. Palevsky, J.-P. Peigneux, M. Spighel, and J.-P. Stroot, *Nucl. Phys.* **A298**, 499 (1978).
- ¹⁹W. Pfeil and D. Schwela, *Nucl. Phys.* **B45**, 379 (1972).
- ²⁰J. T. Londergan, K. W. McVoy, and E. J. Moniz, *Ann. Phys. (N.Y.)* **86**, 147 (1974).
- ²¹I. Blomqvist and J. M. Laget, *Nucl. Phys.* **A280**, 405 (1977).
- ²²These corrections are relatively large here compared to elastic scattering. The main reason is that in elastic scattering the recoil corrections are proportional to momentum transfer and hence small where the cross section is large. Due to the transverse nature of the photon coupling, no factor of momentum transfer appears in the photoproduction case and the correction is correspondingly large [cf. Eqs. (28) and (30)].
- ²³L. M. Saunders, *Nucl. Phys.* **B7**, 293 (1968).
- ²⁴G. Davidson, Ph.D. thesis, Massachusetts Institute of Technology, 1959 (unpublished).
- ²⁵J. W. Staples, Ph.D. thesis, University of Illinois, 1969 (unpublished). We thank M. Blecher for bringing this work to our attention.